Molecular basis for universal HLA-A*0201–restricted CD8$^+$ T-cell immunity against influenza viruses

Sophie A. Valkenburg[a,1], Tracy M. Josephs[b,c,1], E. Bridie Clemens[a], Emma J. Grant[a], Thi H. O. Nguyen[a], George C. Wang[d], David A. Price[e], Adrian Miller[f], Steven Y. C. Tong[g], Paul G. Thomas[h], Peter C. Doherty[a,h,2], Jamie Rossjohn[b,c,e,i], Stephanie Gras[b,c,i,2,3], and Katherine Kedzierska[a,2,3]

[a]Department of Microbiology and Immunology, University of Melbourne, at the Peter Doherty Institute for Infection and Immunity, Melbourne, VIC 3000, Australia; [b]Infection and Immunity Program, Monash University, Clayton, VIC 3800, Australia; [c]Department of Biochemistry and Molecular Biology, Biomedicine Discovery Institute, Monash University, Clayton, VIC 3800, Australia; [d]Division of Geriatric Medicine and Gerontology, Department of Medicine, Johns Hopkins University School of Medicine, Baltimore, MD 21205; [e]Institute of Infection and Immunity, Cardiff University School of Medicine, Cardiff CF14 4XN, United Kingdom; [f]Indigenous Research Network, Griffith University, Brisbane, QLD 4111 Australia; [g]Menzies School of Health Research, Darwin, NT 0810, Australia; [h]Department of Immunology, St Jude Children's Research Hospital, Memphis, TN 38105; and [i]Australian Research Council Centre of Excellence for Advanced Molecular Imaging, Monash University, Clayton, VIC 3800, Australia

Contributed by Peter C. Doherty, February 25, 2016 (sent for review December 22, 2015; reviewed by Christopher Goodnow and Janko Nikolich-Zugich)

Memory CD8$^+$ T lymphocytes (CTLs) specific for antigenic peptides derived from internal viral proteins confer broad protection against distinct strains of influenza A virus (IAV). However, immune efficacy can be undermined by the emergence of escape mutants. To determine how T-cell receptor (TCR) composition relates to IAV epitope variability, we used ex vivo peptide–HLA tetramer enrichment and single-cell multiplex analysis to compare TCRs targeted to the largely conserved HLA-A*0201-M1$_{58}$ and the hypervariable HLA-B*3501-NP$_{418}$ antigens. The TCRαβs for HLA-B*3501-NP$_{418}^+$ CTLs varied among individuals and across IAV strains, indicating that a range of mutated peptides will prime different NP$_{418}$-specific CTL sets. Conversely, a dominant public TRAV27/TRBV19$^+$ TCRαβ was selected in HLA-A*0201$^+$ donors responding to M1$_{58}$. This public TCR cross-recognized naturally occurring M1$_{58}$ variants complexed with HLA-A*0201. Ternary structures showed that induced-fit molecular mimicry underpins TRAV27/TRBV19$^+$ TCR specificity for the WT and mutant M1$_{58}$ peptides, suggesting the possibility of universal CTL immunity in HLA-A*0201$^+$ individuals. Combined with the high population frequency of HLA-A*0201, these data potentially explain the relative conservation of M1$_{58}$. Moreover, our results suggest that vaccination strategies aimed at generating broad protection should incorporate variant peptides to elicit cross-reactive responses against other specificities, especially those that may be relatively infrequent among IAV-primed memory CTLs.

influenza infection | human CD8$^+$ T cells | T-cell receptor

Preexisting CD8$^+$ T-lymphocyte (CTL) immunity directed at peptides derived from internal viral proteins is known to confer protection against specific strains of influenza A virus (IAV) (1–5). Recalled memory CTLs generated by seasonal variants can also expedite virus elimination and host recovery following infection with H1N1, H2N2, H3N2, H5N1, and H7N9 IAVs (2, 3, 6–9). However, it is unclear why such cross-strain responses vary among individuals. The ability of αβ T-cell receptors (TCRαβs) to recognize antigenic epitopes from distinct IAVs and circumvent immune escape relies on peptide sequence conservation and/or structural homology (10–12). A detailed understanding of cross-strain reactivity in relation to defined TCRαβ interactions may therefore inform the rational development of a universal vaccine against IAV.

The conserved HLA-A*0201–restricted M1$_{58–66}$ (GILGFVFTL, referred to hereafter as "M1$_{58}$") (13) and variable HLA-B*07 superfamily-restricted NP$_{418–426}$ (LPFERATVM, referred to hereafter as "NP$_{418}$") (10) peptides are the most immunogenic IAV epitopes described in humans. The M1$_{58}$ epitope has remained unchanged in seasonal and pandemic IAVs since 1918 (1, 8, 14, 15), although viruses with single-alanine-substitution mutants of M1$_{58}$ generated by reverse genetics are replication competent (16). Accordingly, the M1$_{58}$ peptide is an ideal vaccine candidate for >1 billion people globally who express HLA-A*0201. In contrast, the NP$_{418}$ epitope is hypervariable, encompassing >20 different naturally occurring sequences. Analysis of HLA-B*07/B*35–restricted NP$_{418}$-specific CTLs in the wake of the 2009 pandemic revealed at least two distinct responses to this prominent epitope (12).

In this study, we used ex vivo tetramer enrichment combined with single-cell multiplex RT-PCR to dissect TCRαβ signatures within CTL populations specific for the HLA-A*0201-M1$_{58}$ and HLA-B*07/B*35-NP$_{418}$ epitopes. Our data indicate that public A*0201-TCRαβs use molecular mimicry to recognize distinct IAVs.

Results

Natural IAV M1$_{58}$ Variants Emerge in HLA-A2.1 Transgenic HHD Mice. The HLA-A*0201–restricted M1$_{58}$ peptide is broadly conserved across IAVs, although the M1-I2M and M1-L3W variants have been found in 21% of H5N1 sequences (7). Using the influenza resource database at the National Center for Biotechnology Information, we aligned 1,000 full-length sequences representing IAV subtypes infecting different species between 1918 and 2010 to conduct an in-depth validation of M1$_{58}$ conservation.

Significance

Influenza is a rapidly spreading acute respiratory infection that causes profound morbidity and mortality. Established CD8$^+$ T-lymphocyte (CTL) immunity directed at conserved viral regions provides protection against distinct influenza A viruses (IAVs). In this study, we show that public T-cell receptors (TCRs) specific for the most prominent human CTL epitope (M1$_{58–66}$ restricted by HLA-A*0201) are capable of recognizing sporadically emerging variant IAVs. We also identify the structural mechanisms that enable promiscuous TCR recognition in this context. Our analysis suggests that preexisting cross-reactive TCRs may limit the spread of newly emerging pandemic IAVs.

Author contributions: S.A.V., E.B.C., E.J.G., T.H.O.N., G.C.W., P.G.T., P.C.D., S.G., and K.K. designed research; S.A.V., T.M.J., E.B.C., E.J.G., T.H.O.N., S.G., and K.K. performed research; T.M.J., G.C.W., D.A.P., A.M., S.Y.C.T., P.G.T., and J.R. contributed new reagents/analytic tools; S.A.V., T.M.J., E.B.C., E.J.G., T.H.O.N., P.G.T., S.G., and K.K. analyzed data; and S.A.V., T.M.J., E.B.C., D.A.P., A.M., S.Y.C.T., P.G.T., P.C.D., J.R., S.G., and K.K. wrote the paper.

Reviewers: C.G., Garvan Institute; and J.N.-Z., University of Arizona.

The authors declare no conflict of interest.

Freely available online through the PNAS open access option.

Data deposition: Crystallography, atomic coordinates, and structure factors reported in this paper have been deposited in the Protein Data Bank (PDB) database [PDB ID codes 5HHQ (HLA-A*0201-M1-L3W), 5HHP (HLA-A*0201-M1-G4E), 5HHN (HLA-A*0201-M1-F5L), 5HHO (JM22-TCR-HLA-A*0201-M1-G4E), and 5HHM (JM22-TCR-HLA-A*0201-M1-F5L)].

[1]S.A.V. and T.M.J. contributed equally to this study.

[2]To whom correspondence may be addressed. Email: pcd@unimelb.edu.au, stephanie.gras@monash.edu, or kkedz@unimelb.edu.au.

[3]S.G. and K.K. contributed equally to this study.

This article contains supporting information online at www.pnas.org/lookup/suppl/doi:10.1073/pnas.1603106113/-/DCSupplemental.

Table 1. Newly identified naturally occurring $M1_{58}$ peptide variants

GILGFVFTL	Mutant	No.	%	Source	Year	Subtype	Strain
A- - - - - - - -	G1A	1	0.1	Human	2009	H3N2	A/Tomsk/02/2009
W- - - - - - - -	G1W	1	0.1	Swine	2005	H3N2	A/swine/Guangdog/01/2005
-V- - - - - - -	I2V	19	1.9	Avian	1999–2008	H3N2, H5N1, H7N7, H7N2, H7N3, H9N2, H2N1	A/Hanoi/TN405/2005
-M- - - - - - -	I2M*	35	3.5	Avian	1999–2008	H5N1, H6N2, H9N2	A/duck/Hong Kong/140/1998
-T- - - - - - -	I2T	1	0.1	Avian	2002	H5N1	A/duck/Fujian/13/2002
- -W- - - - - -	L3W*	0	0.0	Avian		H5N1	Described in ref. 7
- - -E- - - - -	G4E	1	0.1	Avian	1998	H9N2	A/chicken/Anhui/1/1998
- - - -V- - - -	F5V	2	0.2	Human, avian	1946, 2000	H1N1, H9N2	A/Cameron/1946
- - - -L- - - -	F5L	9	0.9	Human, avian	1983–2009	H1N1, H5N2, H7N3, H11N2	A/Canterbury/236/2005
- - - - -I - - -	V6I	12	1.2	Human, avian	1967–2006	H2N2, H13N6, H1N2, H3N1, H1N1	A/England/10/1967
- - - - - -Y- -	F7Y	1	0.1	Human	1999	H3N2	A/New South Wales/15/1999
Total mutations	82						
Total sequences	998	8.2					

Mutations were found in 8.2% of IAVs, and 11 distinct $M1_{58}$ substitutions were identified across all positions bearing the C-terminal P8 and P9 residues (Table 1). The most frequent $M1_{58}$ mutations occurred at the anchor residue (p2), accounting for nearly 67% of all substitutions in the database (M1-I2M, 42%; M1-I2V, 23%; M1-I2T, 1.2%). Although these $M1_{58}$ variants were detected mainly in avian IAVs (H2, H5, H6, H7, H9, H11, and H13), 8 of the 82 mutant sequences were derived from human isolates.

An established mouse model of IAV escape (17) was used to probe the emergence of $M1_{58}$ mutants. As in humans, the $M1_{58}$ epitope is immunodominant in HLA-A2.1 HHD mice (Fig. S1 *A* and *B*). Amino acid substitutions in $M1_{58}$ were encoded by viral RNA extracted from the lungs of three of seven mice 15 d after infection (Fig. S1 *C–E*), a lower mutation rate compared with the immunodominant H2-$D^b$$NP_{366}$ epitope in WT B6 mice (17). Engineered PR8 viruses carrying the M1-I2M, M1-F5L, M1-V6I, and M1-F7Y mutations grew to similar titers in embryonated eggs and MDCK cell cultures (Fig. S1 *F* and *G*). However, it remains possible that subtle differences in viral fitness may counterselect against $M1_{58}$ mutants in the natural setting. The absence of epitope-specific immune pressure also may lead to the occurrence of viral refugia in individual cases, a phenomenon widely recognized in the ecology field.

Sequence variation within $M1_{58}$ therefore occurs in IAVs recovered from humans (8.2%) and from experimentally infected HLA-A2.1 HHD mice (7.3%). However, unlike the frequent and persistent mutations in NP_{418} (10), these $M1_{58}$ variants are not readily fixed in circulating human IAVs. To determine whether the contrasting patterns of viral variation within $M1_{58}$ and NP_{418} reflect immune selection, we undertook a detailed cellular and molecular evaluation of the corresponding CTL responses.

HLA-A*0201-$M1_{58}^+$ CTLs Are Immunodominant and Recognize $M1_{58}$ Variants. Using direct ex vivo tetramer-based magnetic enrichment (4, 18) to minimize selection bias, we analyzed CTL responses specific for HLA-A*0201-$M1_{58}$ (A2-$M1_{58}$) and HLA-B*3501-NP_{418} (B35-NP_{418}) in individual subjects expressing both HLA-A*0201 and HLA-B*3501 (Fig. 1 and Table S1). A2-$M1_{58}^+$ CTLs were identified with a single conserved tetramer, and B35-NP_{418}^+ CTLs were identified with a tetramer pool corresponding to the main variants from 1918, 1934, 1947, 1980, and 2002 (12). The A2-$M1_{58}^+$ CTL population was consistently larger (17 ± 9.2-fold) than the B35-NP_{418}^+ CTL population (Fig. 1*A*), which frequently predominates in HLA-A*0201$^-$ donors (Fig. S2). Furthermore, the polyclonal A2-$M1_{58}^+$ CTLs recognized all detected mutants, although response frequencies varied and the M1-G4E mutant was weakly immunogenic in five donors (Fig. 1*B*). Conversely, the polyclonal B35-NP_{418}^+ CTLs recognized a limited number of variants (Fig. 1*C*), in line with previous reports of immune escape (10, 12). Thus, $M1_{58}$-specific TCRs cross-react with a broader spectrum of naturally occurring epitope variants compared with NP_{418}-specific TCRs. It is notable in this regard that NP_{418} variants are often composite, incorporating up to three amino acid substitutions, whereas single mutations are more common in $M1_{58}$.

Dissection of A2-$M1_{58}$ and B35-NP_{418} TCRαβ Repertoires. Consistent with previous reports (19–21), direct ex vivo single-cell sequencing of the A2-$M1_{58}^+$ TCRαβ repertoire showed a heavy bias toward T-cell receptor β variable 19 (TRBV19) use across all eight donors, coupled with a dominant T-cell receptor α variable 27 (TRAV27) segment in seven of eight donors (Fig. 2 *A* and *B* and Fig. S3 *A* and *B*). The averaged frequency for TRBV19 was 91.6% (range 44–100%), compared with 49.2% (range 0–91%) for TRAV27. The most common TCRαβ signature was the public clonotype

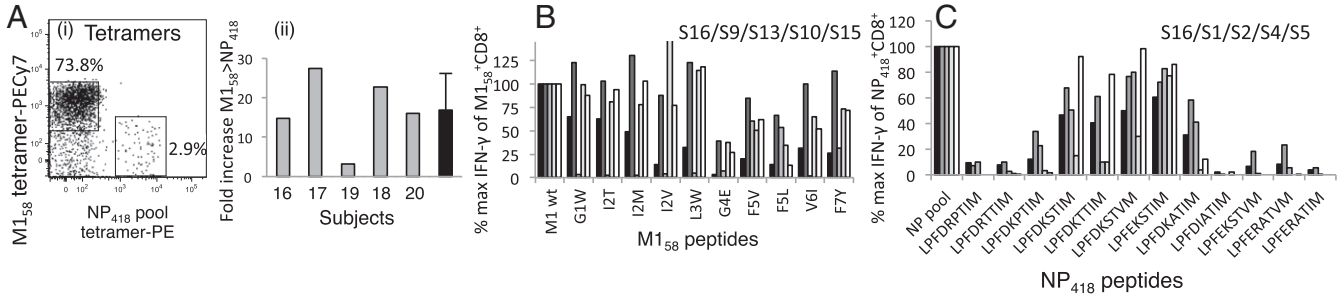

Fig. 1. Ex vivo immunodominance of A2-$M1_{58}^+$ over B35-NP_{418}^+ CTLs. (*A*) Costaining of A2-$M1_{58}^+$ and B35-NP_{418}^+ CTLs directly ex vivo by tetramer enrichment showing (*i*) single tetramer$^+$CD8$^+$CD4$^-$CD14$^-$CD19$^-$ cells and (*ii*) fold-increase of the A2-$M1_{58}$ above the B35-NP_{418} CTL response. (*B* and *C*) Recognition of naturally occurring $M1_{58}$ (*B*) and NP_{418} (*C*) variants by human PBMCs from A2$^+$B35$^+$ donors was assessed 10 d after restimulation using intracellular staining for IFN-γ production in response to the indicated peptides. Data show individual subjects (S).

TRBV19/complementarity-determining region (CDR)3β-SIRSSYEQ paired with TRAV27/CDR3α-GGSQGNL (Fig. 2*C* and Fig. S3 *C*–*E*). In subject 23, the public TRBV19/CDR3β-SIRSSYEQ paired with a similar TRAV27/CDR3α-ASGSSNTGKL (44% of sequences), whereas subject 22 exhibited a limited TCRαβ repertoire in which an alternate TCRβ (TRBV19/CDR3β-GAGGPLNEQ) paired with a non-TRAV27 TCRα (TRAV12.3/CDR3α-SERNNARL). Public TCRαβ clonotypes can therefore be generated in the majority of HLA-A2$^+$ individuals across different ethnicities, including Indigenous Australians.

Reflecting the prevalence of low-frequency private clonotypes, the M1$_{58}$-specific TCRαβ repertoire was more diverse (12.4 ± 6.0 CDR3αβ pairs per donor) than previously reported. Furthermore, the AGA(G$_n$)GG CDR3α motif (22) (in which "$_n$" denotes any number of residues) found by others following long-term culture was not consistently present in our direct ex vivo dataset, although two glycines (GG) featured in 20 of the 45 CDR3α sequences. The CDR3β IRS motif, which forms the basis for "peg–notch" JM22 TCR recognition of the "plain vanilla" M1$_{58}$ epitope (21), was used in 11/45 CDR3β sequences across five donors.

In contrast, analysis of the B35-NP$_{418}^+$ TCR repertoire using pooled B35-NP$_{418}$ tetramers (Fig. S4) revealed distinct CDR3α/CDR3β sequences incorporating diverse TRAV and TRBV segments. A preference for TRBV20-1/TRBJ5-1 rearrangements with a CDR3β length of 7 or 10 amino acids was observed in the TCRβ repertoire, whereas the predominant TCRα chains favored TRAV8-1 and TRAJ18 with a CDR3α length of 8–10 amino acids (Table S2). However, only one common sequence (TRAV8-1/CDR3α-NEGGSTLGRL) was found among individuals (Fig. S4).

There was no overlap between the B35-NP$_{418}^+$ TCR datasets, generating a Morisita–Horn statistic of 1 (zero interindividual similarity). However, the A2-M1$_{58}^+$ TCR datasets overlapped considerably, driven by the public TRBV19/CDR3β-SIRSSYEQ sequence (averaged Morisita–Horn statistic of 0.6). These differences were statistically significant ($P = 0.0056$, Wilcoxon signed tank test). In addition, the Simpson diversity index was higher for B35-NP$_{418}^+$ TCRαβs (0.97 ± 0.03) than for A2-M1$_{58}^+$ TCRαβs (0.75 ± 0.27) (Table S2).

Thus, dominant public TCRαβ clonotypes (TRBV19/TRAV27) are selected in HLA-A*0201$^+$ donors responding to the relatively invariant A2-M1$_{58}$ epitope, whereas TCRαβ clonotypes directed at the hypervariable B35-NP$_{418}$ epitope are more diverse across individuals.

Public M1$_{58}$-Specific TCRαβ Clonotypes Cross-Recognize Newly Identified Variants. How do A2-M1$_{58}^+$ CTLs recognize naturally occurring M1$_{58}$ variants? To investigate this question, peripheral blood mononuclear cells (PBMCs) were stimulated with the mutant peptide (M1-L3W, -G4E, or -F5L) for 10 d and then stained with the M1$_{58}$ WT tetramer. In this way, variant-specific CTLs were amplified by the mutant peptide, and cross-reactive clonotypes identified by reactivity with the M1$_{58}$ WT tetramer were characterized using single-cell CDR3αβ TCR repertoire diversity analysis (Fig. 3 and Table S3). The variant M1-L3W, M1-G4E, and M1-F5L peptides represent naturally occurring M1$_{58}$ mutants, with a CTL response magnitude hierarchy of M1-L3W > M1-F5L > M1-G4E in subject 9 and subject 16 (Fig. 3).

The public HLA-A*0201-M1$_{58}^+$ TCR (CDR3α-GGSQGNL; CDR3β-SIRSSYEQ) recognized all three peptide variants (Table S3), although the frequency was slightly lower for the M1-G4E mutant (47% of the WT). Higher-frequency public TCRαβ use correlated with larger mutant-specific CTL responses (Fig. 1*B*), indicating that public HLA-A*0201-M1$_{58}^+$ TCRs play an important role in variant cross-recognition. Overall, the mutant M1$_{58}$ peptides selected a TCRαβ repertoire comparable to that of WT M1$_{58}$ with similar TRAV27, TRAJ42, TRBV19, and TRBJ2-7 use (except for M1-G4E in subject 16, which used TRAV23DV/6 instead of the typically dominant TRAV27), suggesting that WT HLA-A*0201-M1$_{58}^+$ TCRs are largely cross-reactive with M1$_{58}$ variants.

HLA Presentation and TCR Recognition of M1$_{58}$ Variants. To determine the impact of peptide mutation on HLA binding and T-cell recognition, we assessed the extent to which the naturally occurring M1$_{58}$ mutant peptides M1-F5L, M1-G4E, and M1-L3W stabilize HLA-A*0201. We refolded the HLA-A*0201 molecule with the M1$_{58}$ peptide and each of the three variants to determine the thermal stability of the corresponding peptide-HLA (pHLA) complexes. In complex with the M1$_{58}$ peptide, HLA-A*0201 exhibited a thermal melt point (Tm, the temperature required to unfold 50% of the protein) of ∼66 °C; the Tm was similar for the three M1$_{58}$ variants (Table S4), indicating that the mutations directly affect TCR binding rather than pHLA complex stability.

To understand the mode of recognition of M1$_{58}$ mutants by public HLA-A*0201-M1$_{58}^+$ TCRs, we conducted surface plasmon resonance studies with the previously characterized M1$_{58}$-specific JM22 TCR (TRAV27/CDR3α-AGSQGNL; TRBV19/CDR3β-SSRSSYEQ) (21). We confirmed that the JM22 TCR binds with high affinity (1.79 μM) to the HLA-A*0201-M1$_{58}$ complex (21, 23), but measured substantially lower affinities for the three M1$_{58}$ variants (Table S5). Namely, weak binding (K_d >200 μM) characterized the JM22 TCR interaction with M1-G4E and M1-F5L, and this was further diminished (K_d >600 μM) for M1-L3W, presented by HLA-A*0201 (Table S5). Thus, although the JM22 TCR can recognize all M1$_{58}$ variants, the binding affinity is lower for the mutant epitopes (24).

M1$_{58}$ Variants No Longer Form Plain Vanilla Epitopes. To understand the impact of the naturally occurring M1$_{58}$ mutations on epitope presentation and T-cell recognition, we determined the structures of three binary pHLA complexes (M1-F5L, M1-G4E, and

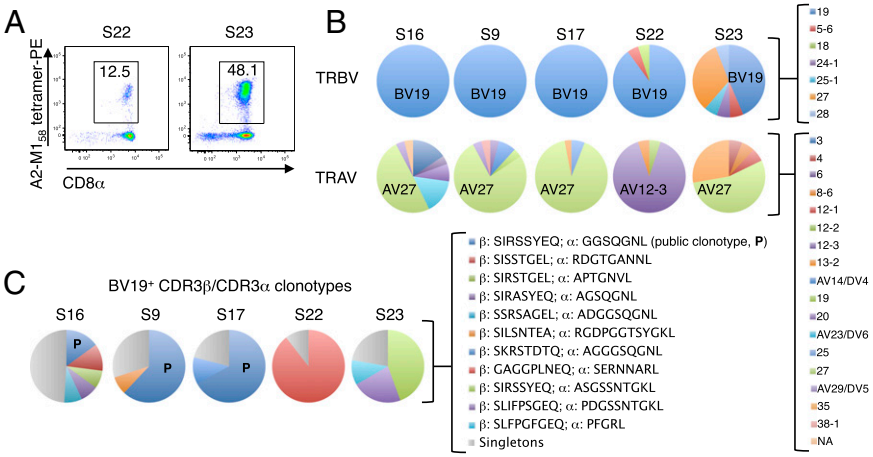

Fig. 2. The A2-M1$_{58}^+$ TCRαβ repertoire is dominated by a public clonotype. A2-M1$_{58}^+$ CTLs were isolated directly ex vivo from non-Indigenous healthy donors ($n = 5$) by magnetic enrichment and flow cytometric sorting of single tetramer$^+$ cells. Populations were gated on viable Dump$^-$tetramer$^+$CD3$^+$CD8$^+$ events. (*A*) Representative flow cytometry profiles showing tetramer$^+$CD8$^+$ T cells after ex vivo enrichment. (*B*) TRBV and TRAV use. (*C*) Frequency of CDR3αβ clonotypes. Corresponding data for healthy Indigenous Australian donors ($n = 3$) are shown in Fig. S3. P, public.

M1-L3W) (Fig. 4 and Table S6) and compared these structures with the previously solved structure of HLA-A*0201-$M1_{58}$ (23). The $M1_{58}$ epitope is considered plain vanilla because the $M1_{58}$ epitope adopts a flat surface in the cleft of HLA-A*0201 (25) (Fig. 4*A*). Indeed, despite containing two aromatic residues (P5-Phe and P7-Phe), these side chains are buried inside the antigen-binding cleft, leaving the P6-Val solvent exposed. The overall structure of the M1-G4E mutant complex is similar to that of the $M1_{58}$ complex, with rmsds of 0.25 Å for the antigen-binding cleft and 0.27 Å for the peptide (Fig. 4*A*). Although the replacement of the glycine residue by glutamic acid does not disturb the backbone conformation for M1-G4E, it allows P6-Val to move deeper into the HLA-A*0201 antigen-binding cleft (Fig. 4*A*). As a result, P5-Phe and P7-Phe are mobile and adopt several conformations, most of which are solvent exposed (Fig. 4*A*).

More dramatic rearrangements were observed for the M1-L3W (Fig. 4*B*) and M1-F5L (Fig. 4*C*) variants. The P3-Leu of the WT $M1_{58}$ peptide is buried in the cleft and interacts with the B pocket of HLA-A*0201, whereas the larger P3-Trp of M1-L3W is accommodated in the B pocket without modification of the overall antigen-binding cleft structure (rmsd of 0.33 Å). However, the M1-L3W peptide must rearrange dramatically due to the presence of the large tryptophan residue at P3 (rmsd of 0.61 Å) (Fig. 4*B*). The P5-Phe side chain swings out of the antigen-binding cleft to avoid steric clashes with P3-Trp and hence becomes solvent exposed. As a consequence, P6-Val is buried in the antigen-binding cleft, and P7-Phe is again mobile and solvent exposed (Fig. 4*B*). Thus, in the HLA-A*0201-M1-L3W structure, the two large aromatic side chains at P5 and P7 are directly available for TCR interaction.

Similarly, the M1-F5L variant adopts a different peptide conformation (rmsd of 0.44 Å) without distorting the antigen-binding cleft (rmsd of 0.29 Å) (Fig. 4*C*). Even though P5-Leu is smaller than P5-Phe, the rotamer of the leucine side chain (like P5-Phe) does not allow docking inside the antigen-binding cleft without changing the overall backbone of the peptide. The P3-Leu therefore no longer interacts with the B pocket of HLA-A*0201 and instead becomes mobile and solvent exposed. The new conformation of the P5-Leu residue also impacts the P6-Val conformation, which becomes buried in the antigen-binding cleft, whereas P7-Phe is now solvent exposed and mobile (Fig. 4*C*).

Overall, these surprising structures of the $M1_{58}$ variants demonstrate that interplay between peptide residues constrains the conformation of the $M1_{58}$ epitope, with any alterations reflecting either the inherent flexibility of particular residues (in M1-G4E and M1-F5L) or steric hindrance (in M1-L3W). As a consequence, single substitutions at different positions in the peptide can transform the plain vanilla $M1_{58}$ epitope into a more featured antigen.

The Public JM22 TCR Recognizes $M1_{58}$ Variants via Induced-Fit Molecular Mimicry. To understand how HLA-A*0201-$M1_{58}^+$ CTLs recognize the naturally occurring epitope variants (Fig. 1*B*), we determined the structures of the JM22 TCR (21) in complex with HLA-A*0201-M1-G4E and HLA-A*0201-M1-F5L (Table S7). As in the WT $M1_{58}$ complex (Fig. 4 *D*–*F*), the JM22 TCR docks orthogonally on the two $M1_{58}$ variant peptides presented by HLA-A*0201 (rmsd of 1.1 Å and 0.7 Å with the M1-G4E and M1-F5L complexes, respectively). The M1-G4E and M1-F5L peptides change conformation upon JM22 TCR binding (Fig. 4 *G* and *H*) to mimic that of the WT $M1_{58}$ peptide (Fig. 4*I*). These structural rearrangements allow key residues (23) from the JM22 TCR β-chain (identified via mutagenesis), namely D32, Q52, and R98, to maintain critical interactions with both the peptide and HLA-A*0201. The requirement for conformational change also explains why the JM22 TCR binds HLA-A*0201-M1-G4E and HLA-A*0201-M1-F5L with lower affinities than HLA-A*0201-$M1_{58}$ (Fig. 4 *G* and *H*).

The leucine substitution at p5 (M1-F5L) is accommodated without rearrangements of the JM22 TCR CDR loops (Fig. 4*J*) (23), whereas the JM22 TCR docking angle is slightly different when in complex with $M1_{58}$ and M1-G4E (78° and 80°, respectively) (Fig. 4 *D* and *F*). This difference is a direct result of the P4-Glu substitution, which causes a 1-Å shift of the CDR3α loop to avoid steric clashes with the P4-Glu (Fig. 4*K*). The key JM22 TCR β-chain residues identified via mutagenesis (23), namely D32, Q52, and R98, conserve their critical interactions with both the peptide and the HLA molecule despite the P4-Glu and P5-Leu substitutions. Thus, the lower affinity of the JM22 TCR for HLA-A*0201-M1-F5L and HLA-A*0201-M1-G4E can be attributed to structural changes in the corresponding peptides, as well as to the CDR3α loop in the case of M1-G4E, following TCR binding (Fig. 4 *G* and *H*, respectively). Given the structural rearrangement of the M1-G4E and M1-F5L peptides, it is anticipated that large changes would occur in the M1-L3W peptide, resulting in an even lower affinity for the JM22 TCR (Table S5).

These ternary structures show that a public TCRαβ can recognize naturally occurring $M1_{58}$ variants via induced-fit molecular mimicry, potentially explaining why this epitope is conserved among influenza viruses circulating in the human population.

Discussion

Diversity in the TCR repertoire has been associated with high-avidity recognition of MHC-peptide antigens, effective viral clearance, and the containment of immune escape (26, 27). In this study, we used a multiplex single-cell RT-PCR (28, 29) to determine whether TCRαβ diversity and/or composition are associated with immune escape in influenza virus infection. The broad recognition spectrum of a public TRAV27/TRBV19$^+$ TCR within the $M1_{58}$-specific CTL repertoire correlated with the relative scarcity of naturally occurring epitope variants. Such public A2-$M1_{58}^+$ TCRs were found to be highly prevalent across donors, including HLA-A*0201$^+$ non-Indigenous donors and Indigenous Australians (HLA-A*0201 frequency of 30–50% and 10–15%, respectively). It is notable in this regard that Indigenous Australians are at greater risk of severe influenza disease, especially when new IAVs emerge (9, 30, 31). Nonetheless, preexisting CTL memory characterized by best-fit public TCRs may confer protection in the context of HLA-A*0201.

The ternary structure of a public TCR bound to the plain vanilla HLA-A*0201-$M1_{58}$ complex (21, 23) showed previously that the central arginine residue within the predominant CDR3β IRS motif (21) is required to allow a peg–notch interaction. We extended this analysis to naturally occurring $M1_{58}$ mutants and found that the

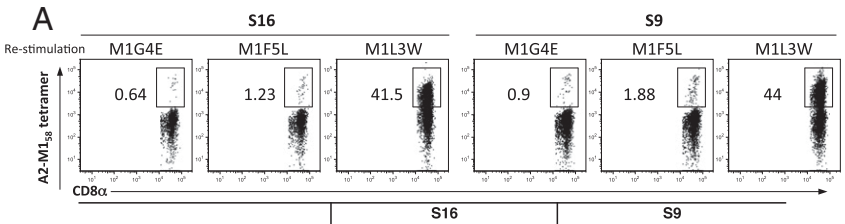

B

	S16				S9			
	M1	G4E	F5L	L3W	M1	G4E	F5L	L3W
Total sequences	26	24	20	16	33	18	20	20
% public TCR usage	15	9	15	19	67	28	45	70
% public TCR usage relative to wt		53.3	100	125		41.4	67.2	104.5

Fig. 3. The A2-$M1_{58}^+$ TCRαβ repertoire cross-recognizes $M1_{58}$ peptide variants. (*A*) A2$^+$ PBMCs were restimulated for 10 d in vitro with the $M1_{58}$ variant peptides M1-G4E, M1-F5L, or M1-L3W and then stained with the $M1_{58}$ WT tetramer. Thus, TCRs were selected to recognize the mutant by the 10-d restimulation and to recognize the cross-reactive WT epitope by tetramer sort. Representative flow cytometry plots are shown gated on CD8$^+$ T cells after the exclusion of CD4$^+$CD14$^+$ CD19$^+$ events. (*B*) Summary of public TCRαβ use.

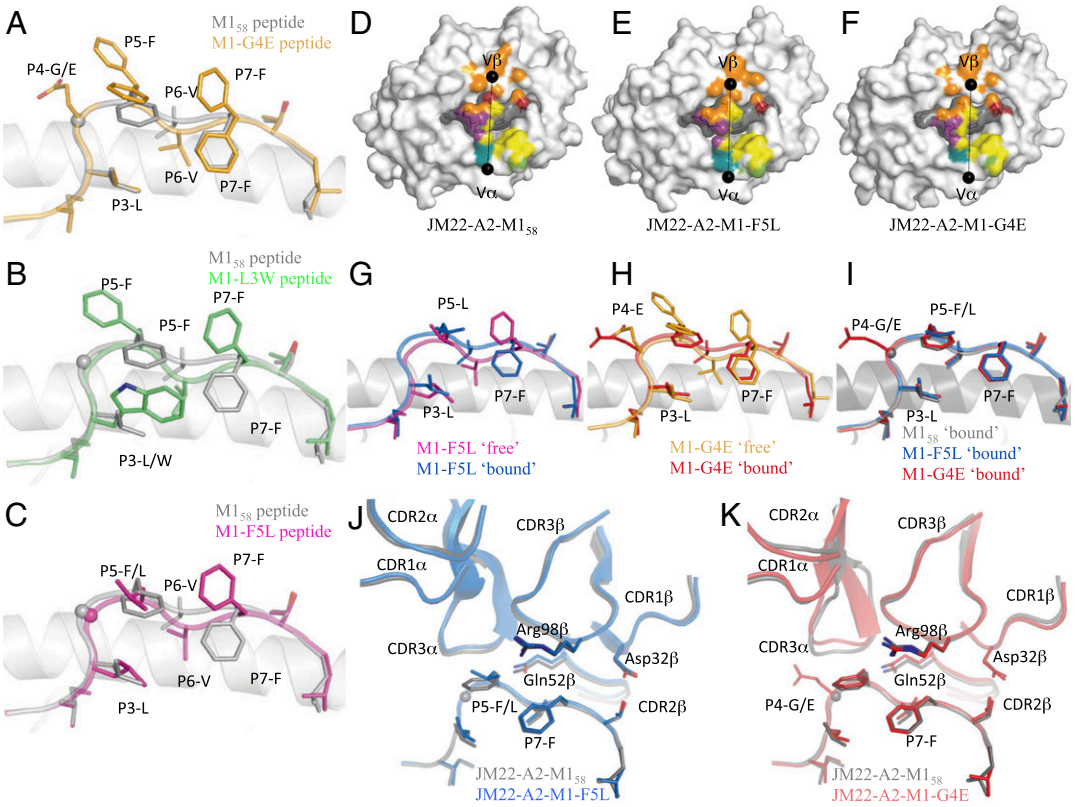

Fig. 4. Structural analysis of M1$_{58}$ variants in complex with HLA-A*0201 and the JM22 TCR. (*A*–*C*) HLA-A*0201 is represented as a white cartoon with the peptide in stick form (M1$_{58}$ in white, M1-G4E in orange, M1-L3W in green, M1-F5L in pink). The glycine Cα is represented as a sphere. (*D*–*F*) The JM22 TCR footprint on the surface of HLA-A*0201 (white) in complex with M1$_{58}$ (*D*), M1-F5L (*E*), and M1-G4E (*F*) peptide (gray). The HLA and peptide atoms are colored teal, green, and purple when contacted by CDR1α, CDR2α, and CDR3α, respectively, and red, orange, and yellow when contacted by CDR1β, CDR2β, and CDR3β, respectively. The black spheres represent the JM22 TCR center of mass for the Vα and Vβ domains. (*G*) Superimposition of HLA-A*0201-M1-F5L free (pink) and bound to the JM22 TCR (blue). (*H*) Superimposition of HLA-A*0201-M1-G4E free (orange) and bound to the JM22 TCR (red). (*I*) Superimposition of HLA-A*0201-M1$_{58}$ (gray), HLA-A*0201-M1-F5L (blue), and HLA-A*0201-M1-G4E (red) bound to the JM22 TCR. (*J* and *K*) Superimposition of JM22 TCR-HLA-A*0201-M1$_{58}$ (dark gray) with the JM22 TCR-HLA-A*0201-M1-F5L (blue) and JM22 TCR-HLA-A*0201-M1-G4E (red) complexes.

same public TCR can recognize naturally occurring variants via induced-fit molecular mimicry, incurring a penalty in terms of binding affinity and T-cell activation. Moreover, the extent of variant recognition correlated with the prevalence of public TCRs, possibly explaining the hierarchical differences in TCR affinity (G4E/F5L > L3W) and T-cell activation (L3W > F5L > G4E). Donors with prominent public TCR use (e.g., subject 9, 67%) recognized the majority of M1$_{58}$ mutants, and the converse was true for donors with limited public TCR use (e.g., subject 16, 15%). These observations suggest that public TCRs may limit, at least to some extent, the establishment of mutant strains within the circulating pool of human IAVs. This idea is consistent with an earlier report in which public Mamu-A*01-CM9$_{181}$–specific TCRs were shown to predict the outcome of simian immunodeficiency virus infection in rhesus macaques (32).

Mutant peptides incorporating substitutions at TCR contact sites within the B35-NP$_{418}$ epitope (reflecting nine decades of natural selection) can be recognized by at least two distinct sets of cross-reactive CTLs specific for either ER or DK motifs at P4-5 (11). In theory, accurate identification of the key solvent-exposed residues and motifs that allow variable peptides to elicit cross-reactive CTL responses could inform the development of rationally designed peptide-mosaic vaccines against unpredicted IAVs (1, 33). Unlike the A2-M1$_{58}^{+}$ CDR3αβ repertoire, however, the NP$_{418}^{+}$ CDR3αβ repertoire in B7^{+} and B35^{+} donors is diverse and private, potentially facilitating the emergence of novel NP$_{418}$ variants. In turn, these mutated epitopes will likely elicit de novo TCR repertoires. Successive waves of variant exposure and diverse TCR recruitment may therefore favor the emergence and perpetuation of NP$_{418}$ mutant IAVs (34).

Structural analyses revealed that single-amino acid substitutions within the M1$_{58}$ peptide can transform this rather flat epitope into conformations that are no longer plain vanilla (25). Although the featureless morphology of HLA-A*0201-M1$_{58}$ determines the character of the highly biased TCR repertoire (21, 25), our data show that structurally prominent M1$_{58}$ variants select a similar array of TCRs. This counterintuitive finding can be explained, at least in part, by the observation that public TCRs (exemplified by JM22) can reshape such variants into conformations that resemble the WT M1$_{58}$ epitope, which is optimal for immediate binding without the need for structural rearrangements. Such induced-fit molecular mimicry was reported previously for an Epstein–Barr virus-specific TCR (35).

In summary, we show here that HLA-A*0201–restricted public TCR clonotypes elicited by the WT M1$_{58}$ epitope can cross-recognize naturally occurring peptide variants. Conversely, the HLA-B*3501–restricted NP$_{418}$ epitope selects a diverse and largely private CDR3αβ repertoire, which correlates with frequent mutational escape and the ongoing circulation of variant IAVs (12, 16). The ability of vaccine-induced CTL responses to protect against variable pathogens should therefore be considered in the context of individual peptides and individual TCRs.

Methods

PBMC Isolation. PBMCs were processed and HLA-typed from randomly selected buffy packs (Melbourne Blood Bank) and healthy donors, with informed written consent (Table S1). Experiments conformed to the National Health and Medical Research Council Code of Practice and were approved by the University of

Melbourne Human Research Ethics Committee and the Human Research Ethics Committee of the Northern Territory Department of Health and Menzies School of Health Research.

Ex Vivo Tetramer Enrichment and Phenotypic Analysis. Lymphocytes (1–8×10^6) were stained with HLA-A*0201-$M1_{58}$ or HLA-B*3501-NP_{418} tetramers conjugated to phycoerythrin (PE) or PE-Cy7. The NP_{418} response was represented by the 1918 (LPFERATIM), 1934 (LPFDRTTIM), 1947 (LPFDKTTIM), 1980 (LPFEKSTVM), and 2002 (LPFEKSTIM) variants (12). Samples were incubated with anti-PE microbeads and tetramer-PE/PE-Cy7$^+$ cells were enriched via magnetic separation (36), then stained with anti–CD4-APC-H7, anti–CD8-PerCP-Cy5.5, anti–CD14-APC-Cy7, anti–CD19-APC-Cy7, anti–CD27-APC, and anti–CD45RA-FITC for 30 min, washed, resuspended, and analyzed/sorted by flow cytometry.

Single-Cell Multiplex RT-PCR. Single tetramer$^+$CD8$^+$CD4$^-$CD14$^-$CD19$^-$ cells were sorted using a FACSAria (BD Biosciences) into 96-well plates. CDR3αβ regions were determined using a single-cell multiplex RT-PCR (28, 29). Sequences were analyzed with FinchTV, and V/J regions were identified by IMGT.

Intracellular Cytokine Staining (ICS). PBMCs were stimulated with peptides for 10 d, and IAV-specific CTLs were quantified using IFN-γ/TNF-α ICS (12, 33). C1R-A*0201 cells, HLA-B*0702$^+$ PBMCs, or C1R-B*3501 cells were used to present antigen. Mouse spleen and bronchoalveolar lavage (BAL) cells were stimulated with $M1_{58}$ (GILGFVFTL), PA_{46} (FMYSDFHFI), or NS_{122} (AIMDKKIIL) for 5 h (17).

HLA-A2.1 Transgenic HHD Mice and de Novo IAV Epitope Mutations. HLA-A2.1 transgenic HHD mice were developed by François Lemonnier (37) and provided by the Pasteur Institute. Experiments were approved by the University of Melbourne Animal Ethics Experimentation Committee. Mice were lightly anesthetized and infected with 10^3 pfu HK (H3N2) virus intranasally. Viral RNA was extracted from lungs 15 d after infection and reverse transcribed to cDNA (17). The M1 region was amplified and sequenced.

Recombinant Influenza Viruses. Influenza viruses with amino acid substitutions in the $M1_{58}$ peptide (M1-I2M, M1-F5L, M1-V6I, and M1-F7Y) were generated using reverse genetics and amplified in embryonated eggs (38).

Protein chemistry and structural biology are described in *SI Methods*.

ACKNOWLEDGMENTS. We thank Nicola Bird for technical assistance and Natalie Saunders for sorting. The C1R-B*3501 plasmid was provided by Dr. David Cole (Cardiff University). HLA-A2.1 transgenic HHD mice were developed and provided by Dr. François Lemonnier (Pasteur Institute). This work was supported by National Health and Medical Research Council (NHMRC) Project Grant 1042662 (to A.M., S.Y.C.T., and K.K.) and NHMRC Program Grant 567122 (to P.C.D. and K.K.). S.A.V. is an NHMRC Early Career Research Fellow, E.B.C. is an NHMRC Peter Doherty Fellow, D.A.P. is a Wellcome Trust Senior Investigator, S.Y.C.T. and K.K. are NHMRC Career Development Fellows, J.R. is an NHMRC Australia Fellow (AF50), and S.G. is an Australian Research Council Future Fellow (FT120100416). E.J.G. is a recipient of an NHMRC Aboriginal and Torres Strait Islander Health Research Scholarship.

1. Quiñones-Parra S, Loh L, Brown LE, Kedzierska K, Valkenburg SA (2014) Universal immunity to influenza must outwit immune evasion. *Front Microbiol* 5:285.
2. Sridhar S, et al. (2013) Cellular immune correlates of protection against symptomatic pandemic influenza. *Nat Med* 19(10):1305–1312.
3. Wang Z, et al. (2015) Recovery from severe H7N9 disease is associated with diverse response mechanisms dominated by CD8$^+$ T cells. *Nat Commun* 6:6833.
4. Valkenburg SA, et al. (2010) Protective efficacy of cross-reactive CD8+ T cells recognising mutant viral epitopes depends on peptide-MHC-I structural interactions and T cell activation threshold. *PLoS Pathog* 6(8):e1001039.
5. Worobey M, Han GZ, Rambaut A (2014) A synchronized global sweep of the internal genes of modern avian influenza virus. *Nature* 508(7495):254–257.
6. McMichael AJ, Gotch FM, Noble GR, Beare PA (1983) Cytotoxic T-cell immunity to influenza. *N Engl J Med* 309(1):13–17.
7. Kreijtz JH, et al. (2008) Cross-recognition of avian H5N1 influenza virus by human cytotoxic T-lymphocyte populations directed to human influenza A virus. *J Virol* 82(11):5161–5166.
8. van de Sandt CE, et al. (2014) Human cytotoxic T lymphocytes directed to seasonal influenza A viruses cross-react with the newly emerging H7N9 virus. *J Virol* 88(3):1684–1693.
9. Quiñones-Parra S, et al. (2014) Preexisting CD8+ T-cell immunity to the H7N9 influenza A virus varies across ethnicities. *Proc Natl Acad Sci USA* 111(3):1049–1054.
10. Boon AC, et al. (2002) Sequence variation in a newly identified HLA-B35-restricted epitope in the influenza A virus nucleoprotein associated with escape from cytotoxic T lymphocytes. *J Virol* 76(5):2567–2572.
11. Berkhoff EG, et al. (2004) A mutation in the HLA-B*2705-restricted NP383-391 epitope affects the human influenza A virus-specific cytotoxic T-lymphocyte response in vitro. *J Virol* 78(10):5216–5222.
12. Gras S, et al. (2010) Cross-reactive CD8+ T-cell immunity between the pandemic H1N1-2009 and H1N1-1918 influenza A viruses. *Proc Natl Acad Sci USA* 107(28):12599–12604.
13. Gotch F, Rothbard J, Howland K, Townsend A, McMichael A (1987) Cytotoxic T lymphocytes recognize a fragment of influenza virus matrix protein in association with HLA-A2. *Nature* 326(6116):881–882.
14. Assarsson E, et al. (2008) Immunomic analysis of the repertoire of T-cell specificities for influenza A virus in humans. *J Virol* 82(24):12241–12251.
15. Tu W, et al. (2010) Cytotoxic T lymphocytes established by seasonal human influenza cross-react against 2009 pandemic H1N1 influenza virus. *J Virol* 84(13):6527–6535.
16. Berkhoff EG, et al. (2005) Functional constraints of influenza A virus epitopes limit escape from cytotoxic T lymphocytes. *J Virol* 79(17):11239–11246.
17. Valkenburg SA, et al. (2013) Acute emergence and reversion of influenza A virus quasispecies within CD8+ T cell antigenic peptides. *Nat Commun* 4:2663.
18. Moon JJ, et al. (2007) Naive CD4(+) T cell frequency varies for different epitopes and predicts repertoire diversity and response magnitude. *Immunity* 27(2):203–213.
19. Moss PA, et al. (1991) Extensive conservation of alpha and beta chains of the human T-cell antigen receptor recognizing HLA-A2 and influenza A matrix peptide. *Proc Natl Acad Sci USA* 88(20):8987–8990.
20. Lawson TM, et al. (2001) Influenza A antigen exposure selects dominant Vbeta17+ TCR in human CD8+ cytotoxic T cell responses. *Int Immunol* 13(11):1373–1381.
21. Stewart-Jones GB, McMichael AJ, Bell JI, Stuart DI, Jones EY (2003) A structural basis for immunodominant human T cell receptor recognition. *Nat Immunol* 4(7):657–663.
22. Naumov YN, et al. (2008) Multiple glycines in TCR alpha-chains determine clonally diverse nature of human T cell memory to influenza A virus. *J Immunol* 181(10):7407–7419.
23. Ishizuka J, et al. (2008) The structural dynamics and energetics of an immunodominant T cell receptor are programmed by its Vbeta domain. *Immunity* 28(2):171–182.
24. Rossjohn J, et al. (2015) T cell antigen receptor recognition of antigen-presenting molecules. *Annu Rev Immunol* 33:169–200.
25. Davis MM (2003) The problem of plain vanilla peptides. *Nat Immunol* 4(7):649–650.
26. Messaoudi I, Guevara Patiño JA, Dyall R, LeMaoult J, Nikolich-Zugich J (2002) Direct link between mhc polymorphism, T cell avidity, and diversity in immune defense. *Science* 298(5599):1797–1800.
27. Price DA, et al. (2004) T cell receptor recognition motifs govern immune escape patterns in acute SIV infection. *Immunity* 21(6):793–803.
28. Wang GC, Dash P, McCullers JA, Doherty PC, Thomas PG (2012) T cell receptor αβ diversity inversely correlates with pathogen-specific antibody levels in human cytomegalovirus infection. *Sci Transl Med* 4(128):128ra42.
29. Nguyen TH, et al. (2014) Recognition of distinct cross-reactive virus-specific CD8+ T cells reveals a unique TCR signature in a clinical setting. *J Immunol* 192(11):5039–5049.
30. Flint SM, et al. (2010) Disproportionate impact of pandemic (H1N1) 2009 influenza on Indigenous people in the Top End of Australia's Northern Territory. *Med J Aust* 192(10):617–622.
31. Clemens EB, et al. (November 17, 2015) Towards identification of immune and genetic correlates of severe influenza disease in Indigenous Australians. *Immunol Cell Biol*, 10.1038/icb.2015.93.
32. Price DA, et al. (2009) Public clonotype usage identifies protective Gag-specific CD8+ T cell responses in SIV infection. *J Exp Med* 206(4):923–936.
33. Valkenburg SA, et al. (2011) Immunity to seasonal and pandemic influenza A viruses. *Microbes Infect* 13(5):489–501.
34. Wahl A, et al. (2009) T-cell tolerance for variability in an HLA class I-presented influenza A virus epitope. *J Virol* 83(18):9206–9214.
35. Macdonald WA, et al. (2009) T cell allorecognition via molecular mimicry. *Immunity* 31(6):897–908.
36. Valkenburg SA, et al. (2013) Preemptive priming readily overcomes structure-based mechanisms of virus escape. *Proc Natl Acad Sci USA* 110(14):5570–5575.
37. Pascolo S, et al. (1997) HLA-A2.1-restricted education and cytolytic activity of CD8(+) T lymphocytes from beta2 microglobulin (beta2m) HLA-A2.1 monochain transgenic H-2Db beta2m double knockout mice. *J Exp Med* 185(12):2043–2051.
38. Kedzierska K, et al. (2008) Complete modification of TCR specificity and repertoire selection does not perturb a CD8+ T cell immunodominance hierarchy. *Proc Natl Acad Sci USA* 105(49):19408–19413.
39. Gras S, et al. (2009) The shaping of T cell receptor recognition by self-tolerance. *Immunity* 30(2):193–203.
40. Gras S, et al. (2009) Structural bases for the affinity-driven selection of a public TCR against a dominant human cytomegalovirus epitope. *J Immunol* 183(1):430–437.